The Spiral as a Traveling Wave Structure for Broadband Antenna Applications

JOHNSON J. H. WANG
Wang Electro-Opto Corporation
Marietta, Georgia, USA

The spiral has been limited to applications for receive only because it is invariably loaded dissipatively, with a typical 3-dB loss and the resulting low efficiency. In this article, we treat the spiral as a traveling-wave (TW) structure that has unique ultra-broadband, complex, multi-facet radiation characteristics, and report development of spirals with efficient transmit performance suitable for all applications such as telecommunications and radar. Its excellent form factor and its size reduction potential are discussed. The spiral's unique geometry is also shown to allow easy and powerful switching, control and various manipulations, etc., to achieve performance and special features that are difficult or even impossible by antennas of other geometries. These unique multimode, multi-polarization, and inherent phase patterns are utilized to achieve ultra-broadband phased arrays and smart antennas for applications involving multifunction, real-time switched modes, among others.

Introduction

The spiral is a traveling wave (TW) structure that has unique, complex, multifacet radiation characteristics that have made it an important antenna for military applications in broadband radar warning, electronic countermeasure, direction finding, etc., in which the spiral antenna is used for receive only, with its broadband pattern quality being of primary importance and its gain and efficiency being of secondary consideration. However, for other applications, such as telecommunications and radars, which require efficient transmit performance, spiral antennas have not been deployed because they are invariably loaded dissipatively, with a typical 3-dB loss and the resulting low efficiency.

Among broadband antennas, the spiral enjoys the advantages of small size and conformability, but also a unique form factor making it compatible with the platform on which it is mounted. These physical features are of utmost practical importance, especially for frequencies at the C-band and lower, where the wavelength is significant with respect to dimensions of humans and their equipment. As a result, the spiral antenna has become the only airborne antenna in use for military applications that require ultrawide bandwidth. Driven by these military needs, the spiral as a receive antenna has been extensively researched and highly perfected, achieving excellent multimode pattern performance over multioctave bandwidths.

Although the progress has been underreported in the open literature due to its exclusively military applications, the book by Corzine and Mosko (1990) provided fairly extensive coverage on the subject, including some crucial practical aspects of the spiral antenna most vital to applications. We will not elaborate on these receive-only spiral antennas except to emphasize the fact that their ultrawideband characteristics are rooted in their TW heritage.

With the advent of the Information Age, the need for broadband and multiband telecommunication has propelled enormous research activities in the last decade to develop broadband/multiband radar and telecommunications antennas. Meanwhile, the electronics industry has been making a feverish, broad-front, and highly successful drive toward miniaturization of hardware during the past half-century, epitomized by the sustained legendary advances in IC (integrated circuits) devices well characterized by the so-called Moore's law. Driven by these two thrusts, the lack of broadband miniaturized antennas now stands out as a fundamental technical barrier in wireless telecommunications.

Not widely recognized is the fact that, during the last decade, high-efficiency spiral antennas were being developed for wideband performance by Wang and Tripp (1991, 1994, 1996a, 1996b), Wang and Tillery (1996), Wang et al. (1996), and Wang (1997), and for narrow-band applications by Nakano et al. (1986). In their approaches, the conventional dissipative loading in the TW structure is replaced by a conducting ground plane below one side of the spiral. As a result, high-efficiency (low-loss) radiation and platform-compatibility are both achieved, and at low manufacturing costs. This paper is focused on spiral antennas of the wideband type. It is intended to provide a bird's-eye view of high-efficiency wideband spiral antennas suitable for transmit as well as receive, as needed in radar and telecommunications applications. Common features shared by the receive-only spiral antennas and the high-efficiency telecommunications spiral antenna will be mostly skipped since they are covered by other papers in this special issue on spirals.

TW Antennas Are Inherently Broadband

As defined by Walter (1965), a *TW antenna* is an antenna for which the fields and currents that produce the far fields can be represented by a TW. Radiation takes place in a TW antenna, as part of the TW process, generally in a smooth and continuous manner; as a result, the TW antennas are inherently broadband, with the spiral having the largest bandwidth. If an antenna has two TWs of comparable amplitudes and traveling in opposite directions, they become a standing wave; in this case the antenna is called a *standing wave antenna*. The standing wave antenna does not transmit efficiently except at resonant frequencies at which the two TWs contribute positively to the far field, since the far-field effects of these two TWs generally nullify each other. As a result, standing wave antennas operate only at their resonant frequencies, which are dependent on the physical dimensions of the antenna, and thus are commonly called *resonant antennas*. Consequently, the resonant antenna is recognized, by connotation as well as by definition, as a narrow-band device. For resonant antennas, impedance matching techniques would have only limited effect on broadening of their bandwidth, as will be discussed in what follows.

Let us first limit the present discussion to the simpler case of a transmit antenna, in which case the antenna viewed by the source can be represented by a simple Thevinin's or Norton's equivalent two-terminal network consisting of a reactive element, a radiation resistance, and a dissipative resistance. (In the case of a receive antenna, a complex bridge network is needed to represent the antenna.) In the theory of network analysis and synthesis, the subject of bandwidth has been extensively studied and well understood. The fundamental physical limitation on broadband matching for networks has been well established and was first extended to antennas by Chu (1948).

Bandwidth and efficiency of transmission are exchangeable quantities in impedance matching of a load having a reactive component. Reactive and resistive elements are gener-

ally frequency dependent, with the resonant antennas having highly variable reactance and radiation resistance. The broad impedance bandwidth of the TW antenna is due to its fairly stable radiation resistance and low reactance.

The reason why the TW antenna has an inherently stable radiation resistance and a low reactance can be explained simply by the fact that radiation either is a continuation of the TW or takes place during propagation of the TW in the antenna aperture. That this happens in turn depends on the efficient launch and support of a TW on the antenna structure. For example, the Yagi–Uda array and the log-periodic (LP) dipole array are both end-fed TW arrays, but the former had a narrow bandwidth of 2% when it was invented while the latter has ultrawide bandwidth (up to 1000%). Even though they have a similar structure, differing only in the length, location, excitation, and number of the individual dipoles in the array, the TW is efficiently launched in the Yagi–Uda antenna only over a narrow bandwidth. It is revealing to view both antennas as TW arrays of dipoles, with the broadband performance of the LP array achieved by broadband propagation and radiation of the TW.

A broadband antenna must exhibit not only a fairly stable and resistive impedance, but also a fairly consistent radiation pattern, over the frequency range of operation. Fortunately, the radiation of a TW antenna is either a continuation of the TW, as in the case of the LP array, or an action taking place along the path of the TW in the antenna aperture, as in the case of the spiral. Both are inherently stable broadband processes.

Theoretical Basis for the Spiral's Ultrawide Bandwidth

The invention of the high-efficiency spiral-mode microstrip (SMM) antenna (Wang & Tripp, 1991, 1994) was partially inspired by the evolution of the Yagi–Uda antenna into the LP array. A basic description of this antenna can be found in Wang & Tripp, 1991, but significant advances, which can also be found in the literature, have been made since then. Figure 1 shows the basic configuration of the SMM antenna, in which the thickness d can be as small as 0.02 λ, where λ is the operating wavelength (at the lowest frequency of the operating band).

Before the invention, the spiral was used and viewed by engineers solely from the perspective of receive-based applications. Even today, many engineers are still comparing the SMM antenna with the conventional direction-finding spiral antennas, failing to do justice to its merits as a telecommunications and radar antenna.

Figure 1. Top and cross-sectional views of the SMM antenna.

That the narrow-band Yagi–Uda antenna evolved into the LP dipole array, which became the first ultrawideband antenna widely used for telecommunications, is truly remarkable and inspiring and serves to illustrate the potential broad bandwidth of the TW antennas in general. It has been noted that, in the case of the LP array, if a TW could be efficiently supported in a structure over a broad bandwidth, with capability for efficient and stable radiation as well, it would constitute an ultrabroadband antenna. Now, the spiral antenna with a lossy cavity to dissipate all the undesired power on the other side has been well developed. If one could launch TW on a spiral with mode purity without the dissipative cavity, the TW would then be able to radiate efficiently (a point to be explained later), and the antenna would become an ultrabroadband high-efficiency antenna suitable for transmit.

Furthermore, it has been noted that an SMM antenna also has an open, accessible geometry and structure like the Yagi–Uda antenna, thus it could be broadbanded in a manner similar to the way the narrow-band Yagi–Uda antenna evolved into the ultrawideband LP dipole array. We also recognized the advantage of the SMM antenna over the LP array in its smaller size and platform compatibility, which have profound practical importance.

The ultrabroadband impedance of a variety of spiral structures has been well established by several theories, among the most fundamental and useful of which is that based on planar self-complementary structure (Deschamps, 1959). For nonzero modes of an N-terminal self-complementary antenna of infinite extent, the impedance Z between each terminal and a common point at the center of the self-complementary structure is a frequency-independent constant equal to

$$Z = \frac{30\pi}{\sin\left(\dfrac{\pi m}{N}\right)} \text{ ohms,} \tag{1}$$

where the nth terminal ($n = 1, 2, \ldots, N$) is fed by a voltage $Ve^{\pm(j(2mn\pi/N))}$, and m is the mode number. Based on experimental observation, the impedance of nonzero spiral modes for the SMM antenna is close to the impedance of the free-standing self-complementary antenna given above.

The TW approach is less abstract and mathematical, providing more comprehensible underlining physics for the spiral antenna, and is presented here to provide an insight into the inherent wideband characteristics demonstrated in the experimental results to be displayed later in this paper. This insight should also help to guide researchers in exploring and fulfilling the potential of the spiral in antenna applications.

From the viewpoint of TW, the spiral, including the necessary ground plane and the substrates (dissipative or nondissipative) between them, constitutes slot lines, microstrip lines, etc., efficient for TW propagation with fairly stable impedance over multioctave bandwidth. Impedance matching based on the TW consideration in conjunction with (1) has been found to be quite useful. Most of the problems in impedance matching are in designing a wideband feed network to support the desired spiral modes.

The radiation of the TW along the spiral is rooted in its unique mechanism for radiation, which can be demonstrated as follows. The radiated electric field of an antenna, such as the SMM antenna shown in Figure 1, is given by the well-known integral equation

$$\mathbf{E}(\mathbf{r}) = \int_S [-j\omega\mu_0 \{\boldsymbol{n}' \times \mathbf{H}(\mathbf{r}')\} g(\mathbf{r}, \mathbf{r}') + \{\boldsymbol{n}' \times \mathbf{E}(\mathbf{r}')\} \times \nabla' g(\mathbf{r}, \mathbf{r}') \tag{2}$$

$$+ \{\boldsymbol{n}' \cdot \mathbf{E}(\mathbf{r}')\}] \nabla' g(\mathbf{r}, \mathbf{r}') \, ds',$$

where S is an arbitrary surface enclosing the antenna; **r** and **r**′ are field and source position vectors, respectively; and **n**′ denotes an outward unit vector perpendicular to the surface S' at a source point **r**′.

In the case of the planar spiral S, as shown in Figure 1, the radiation for the half-space $z \geq 0$ can be viewed as due to the sources on an infinite half-plane $z = z_1$ located at an arbitrary z_1 above the spiral. The integrand in (2) can be simplified, for the case of a half-space, to a single term containing only an equivalent magnetic current $2n' \times E(\mathbf{r}')$. If the spiral is truncated, then the surface S would become a disk-shaped closed surface enclosing the spiral.

In plain words, this equation shows that the electric-field intensity $E(r)$ at a field point r is a function of the fields $E(r')$ and $H(r')$ at the source point r' in the source region specified by the surface S enclosing the antenna. This mathematical expression is equivalent to Huygens's principle, which states that the wave front at a point can be considered as a new source of radiation.

Let us assume that a single time-harmonic TW travels along the spiral arms, resulting in an electrical field E given by

$$E = A(\rho)\, e^{jm\phi} \qquad \text{at } z = d \qquad (3)$$

for a given m, where ρ, ϕ, and z are the cylindrical coordinates. Equation (3) can be viewed as the defining equation for the spiral mode m. E is the field that gives rise to radiated fields in the far zone.

Extensive experimental data exist to support the validity of this assumption for a well-designed spiral antenna with mode purity. By substitution of (3) into (2), the radiated field in (2) would have an $\exp(jm\phi)$ variation in its radiation pattern. The basic pattern of this spiral antenna for modes $m = 0, 1, 2, 3$ are shown in Figure 2 as a function of angle θ. For most applications, the mode-1 ($m = 1$) case is of primary interest, but other modes have been found to have important applications, as will be discussed later. In most applications, a pure single mode is needed; in such a case we observe that as long as there is only a single TW mode, $m = m_0$ ($m < 4$), in the spiral antenna, the far field would have one of the four ideal patterns corresponding to the mode number m_0.

Next we discuss the concept of the radiation zone, which is a very useful approximate concept for the design of spiral antennas. For antenna radiation to be effective, the radiated fields at r due to individual sources at points r' over the antenna must have a fairly uniform phase, so that their cumulative effects can lead to a maximum field intensity with minimal phase cancellation among them. In the case of a spiral, this happens for sources at its "radiation zones" (as shown in Figure 3 for the $m = 1$ mode), which are circular rings with circumference of $m\lambda_p$ (or diameter of $m\lambda_p/\pi$), where m is the mode of operation (an integer) and λ_p is the propagating wavelength. In the radiation zone the source field $E(r')$ in one turn of the
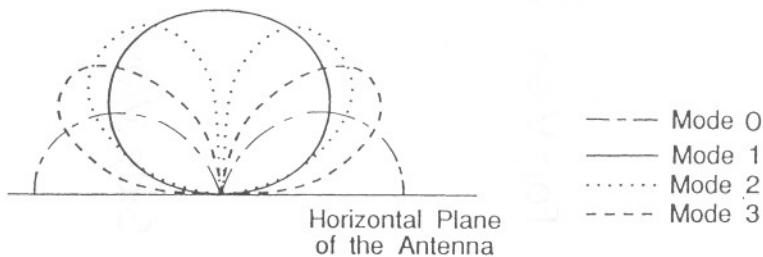

Horizontal Plane
of the Antenna

— – — Mode 0
——— Mode 1
········ Mode 2
– – – – Mode 3

Figure 2. The basic patterns of spiral modes 0, 1, 2, and 3.

Top View

Radiation zone $\left(\rho_r \sim \lambda/2\pi\right)$

ρ_r

$\rho \rightarrow$

Current density

0

ρ_r

ρ

Side View

Spiral

Outgoing wave

Reflected wave
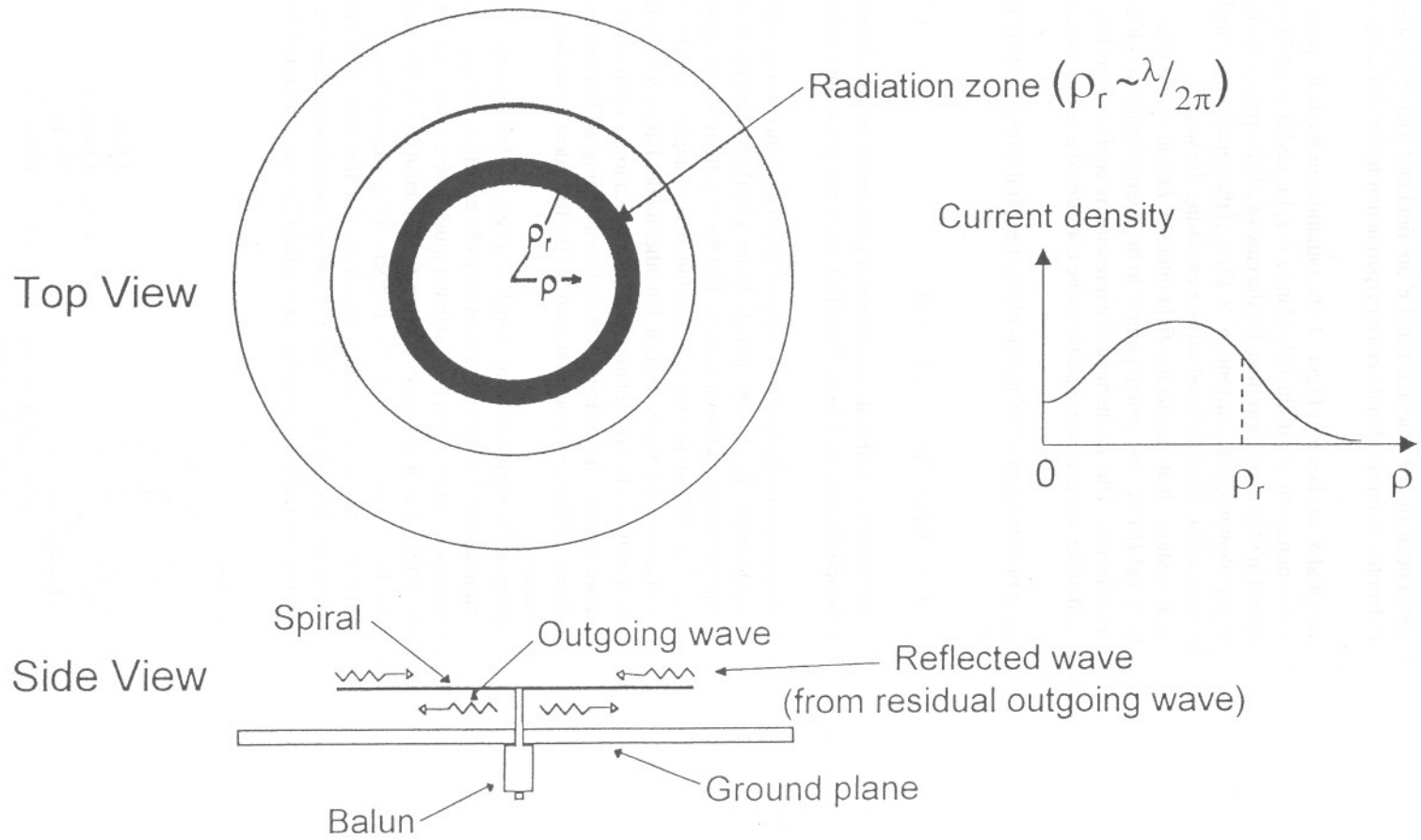(from residual outgoing wave)

Ground plane

Balun

Figure 3. The radiation zone of a spiral antenna.

spiral arm is closely in phase with that in the next turn, and thus they both contribute positively and cumulatively to the radiated fields. Outside the radiation zone, the sources contribute to the far fields in an incoherent manner, giving rise to minimal radiated field intensity.

As a result, the radiation of such an antenna can be approximately given by replacing the domain of the integration, *S*, in (2) by an appropriately chosen radiation band, ΔS, which is the circumferential area adequately specifying the region containing the equivalent magnetic current for the spiral antenna. That is,

$$\mathbf{E(r)} \sim \int_{\Delta S} [\ ] \ \nabla' \mathbf{g(r, r')} \ ds' \tag{4}$$

It can also be shown that such a loop current (representing the source current in the radiation zone) having a constant amplitude and a phase variation of exp(j*m*φ) would have a general radiation pattern given by Figure 2 for mode *m*, regardless of the diameter of the radiation zone.

It is worth pointing out that, to our knowledge, no exact mathematical solution exists for wave problems involving a spiral geometry. As a comparison, physical problems formulated in differential equations with boundary conditions involving canonical geometries such as spheroids, cylinders, and planes have extensive solutions using mathematical functions such as transcendental functions, Bessel functions, and spheroidal wave functions.

While an exact mathematical solution is at present unattainable, engineers have attempted approximate solutions by the following methods:

- Approximation of the spiral geometry and source by methods that are amenable to solution methods developed for canonical geometries. (This approach could miss the essence of the spiral.)
- Asymptotic and quasi-static solution, alone or in combination. (While useful for certain features, these methods have very large blind spots.)
- Numerical solution using a digital computer. (The spiral is probably the most difficult antenna problem to tackle by this approach because if the spiral arms must be discretized, the spiral antenna can be electrically so large as to be computationally impossible for modern computers, including the supercomputer, because of the computational round-off errors and limited speed and memory.)
- Empirical formulas.

It must be emphasized that, from the perspective of TW, the experimental results suggest that existing analysis techniques are inadequate to address the problem thoroughly to uncover the possible truly unique and fundamental characteristics rooted in the spiral geometry.

Experimental Observations and Applications

Much of the recent success in the development of high-efficiency spiral antennas can be well explained by the above theory rooted in the premises that properly generated spiral modes are TWs propagating along the spiral arms; more specifically, a properly generated and guided spiral-mode wave does follow the path of the spiral arms as a TW. This is an extremely crucial point that many researchers have not yet closely followed and, more importantly, taken advantage of, even though general observations like this have been noted for over two decades.

The spiral as a TW structure has unique, complex, multifaceted radiation characteristics amenable to tuning. The spiral is also physically smaller and more compact than other TW antennas. The compactness of the spiral antenna is, obviously, due to the fact that its TW propagates in a manner that is most efficient in the use of space. This unique feature of compactness of the spiral for supporting TW modes has already been recognized and exploited in microwave circuit designs, in which inductors and delay lines formed by spirals are widely used. The compactness of the spiral as compared with other TW antennas cannot be overemphasized since antenna size reduction is now recognized as one of the three fundamental technological barriers in wireless telecommunication.

These high-efficiency spiral antennas using no dissipative loading, or using minimal dissipative loading at the edge (rim) of the spiral structure, have been found to be useful for applications in telecommunications and radars, especially when ultrawide bandwidth, low profile, and platform compatibility are required. This new movement represents a fundamental departure from the traditional cavity loading approach used in planar and conical spirals.

Mode 1

Extensive experimental data exist that demonstrate the ultrabroadband and high-efficiency performance achieved by the mode-1 SMM antenna. Measured voltage standing wave ratio (VSWR) for an SMM antenna of 2.5-inch diameter and 0.2-inch thickness on a ground plane of 5-inch diameter is shown in Figure 4 over a 2–18 GHz bandwidth. The rotating-linear patterns for this antenna are shown in Figures 5(a)–5(c). A 10:1 bandwidth has been achieved by some models, and bandwidth up to 30:1 is also feasible in principle.

In comparing the SMM antenna with the conventional cavity-loaded spiral, one must be aware of the fact that the nice patterns for the latter are invariably recorded by mounting the antenna on a metallic cylinder of the same diameter, so that the spiral is, in effect, mounted on the top surface of the cylinder. This allows the conventional cavity-loaded spiral to have low ripple and low axial ratio in its pattern; however, this also means its pattern will be disrupted when mounted on a platform, usually flush-mount or with low protrusion. The SMM antenna has a built-in ground plane; as a result, it is platform compatible, with no degradation in pattern from the data shown when mounted on a platform. It is fairly insensitive to the ground plane on which it is mounted because its mode-1 pattern drops sharply near the horizon (the horizon is generally parallel to the surface of the ground plane). Therefore, once an SMM antenna breadboard is successfully designed for a given ground plane, it is fairly easy to transition it to a field model with virtually no degradation in performance.

It is worth commenting that some researchers have had difficulties in obtaining the fine experimental results obtained for tens of models by this author and his associates, either experimentally or by computer analysis, for the mode-1 spiral as well as the mode-0 spiral discussed in the following subsection. As for computer analysis, its accuracy is limited because the spiral is, in essence, an electrically large structure if one discretizes it in full consideration of the individual spiral arms, as discussed earlier. As for the experiments, the difficulties are mainly in launching and maintaining the desired spiral modes.

In general, the spiral geometry per se is not too crucial for the design, and is selected in consideration of performance goals. For example, when high gain is desired, a coarser spiral width or a certain equiangular/log-periodic arm width expansion should be selected. The ground plane size is generally at least large enough to cover the radiation zone for the lowest operating frequency, and preferably twice as large or larger. For the SMM antenna, the permittivity of the spacing between the spiral and the ground plane is low, and it is easiest to match when the dielectric constant is near unity.
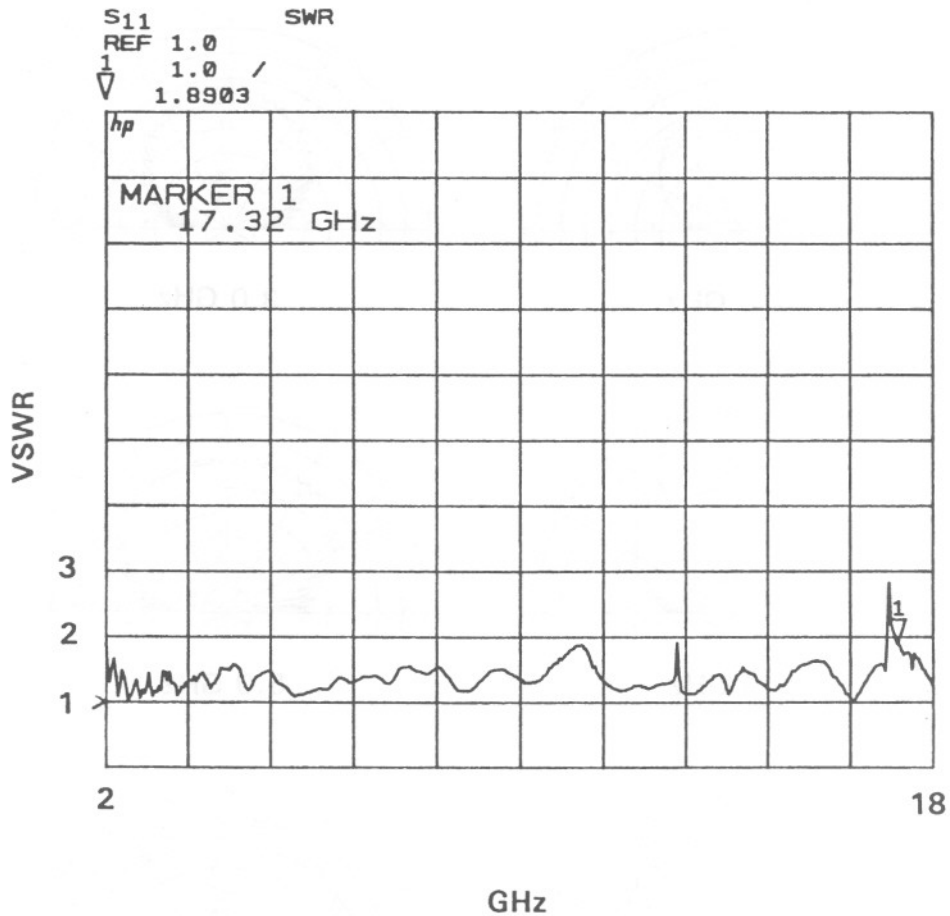
Figure 4. Measured VSWR over 2–18 GHz for the SMM antenna in Figure 1.

In most cases the failure to launch and maintain the desired traveling wave is rooted in the design of the feed network, which in the simple case of a two-arm spiral is a balun. The purpose of the balun is to transform the unbalanced mode of a typical feed cable, often 50 ohms, to a balanced mode of propagation with an impedance significantly higher in order to match for the high impedance of the spiral antenna.

The SMM antenna is notoriously unforgiving when an improper feed network is used. This is in sharp contrast to the cavity-loaded spiral or a spiral with a ground plane placed at $\frac{1}{4}$-wavelength behind it. The absorbing material in the cavity and the tuning effect of the reflector would mitigate and compensate for the effects of a bad feed, allowing the antenna to achieve at least some encouraging performance, upon which the engineer can refine further. In the case of the SMM antenna, a bad feed can lead to disastrous results that offer no clue, nor encouragement, for possible improvement. This is why the discovery of the SMM antenna did not happen until three decades after earlier experiments (e.g., Kaiser, 1960; Donnellan, 1960). Similarly, theoretical studies tended to overlook proper specification of the excitation fields. Often an oversimplified excitation field is specified—a practice by analysts of the spiral as well as most other antennas—thus missing a crucial and essential ingredient for proper launching of the desired traveling waves.

2.0 GHz   3.0 GHz

4.0 GHz   5.0 GHz

6.0 GHz   7.0 GHz
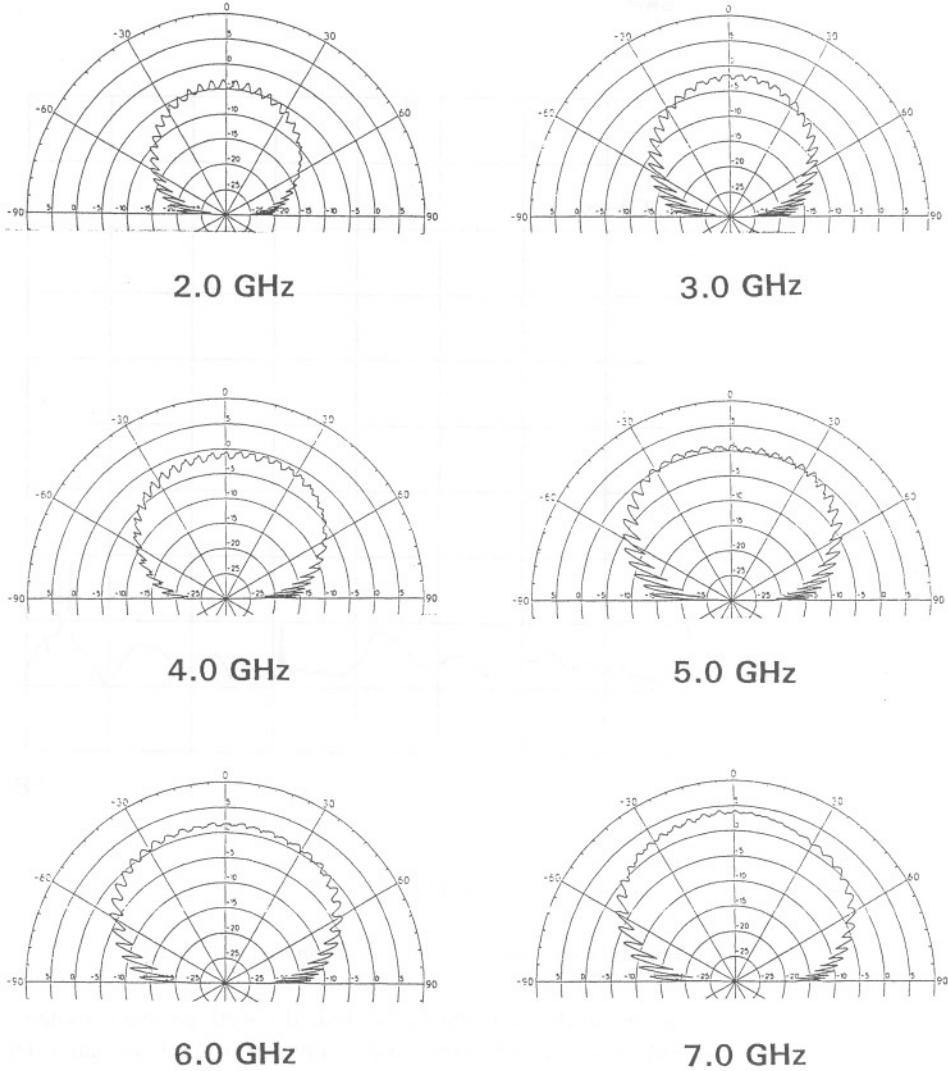
Figure 5(a). Measured rotating-linear patterns of an SMM antenna in Figure 1.

Mode 0

The spiral modes, specifically modes 1, 2, and 3, have been known for four decades and have been well exploited in the widely used cavity-loaded spiral antennas. As discussed earlier, until recently, the universal approach to achieving broad bandwidth has been to place behind the spiral a cavity loaded with absorbing materials to dissipate radiation on this side of the spiral. For mode 2, the use of a small ground plane (with a circumference smaller than $2\lambda_1$, where λ_1 is the free-space wavelength of the lowest operating frequency) placed closely behind the spiral has been studied by several researchers (Kaiser, 1960; Donnellan, 1960; Yamauchi et al., 1994). They reported that when both arms of a two-arm spiral are excited in equal amplitude and phase, with the closely spaced small conducting plate serving as ground for the excitation voltage, mode 2 radiation was observed over an apparently

8.0 GHz

9.0 GHz

10.0 GHz

11.0 GHz

12.0 GHz

13.0 GHz
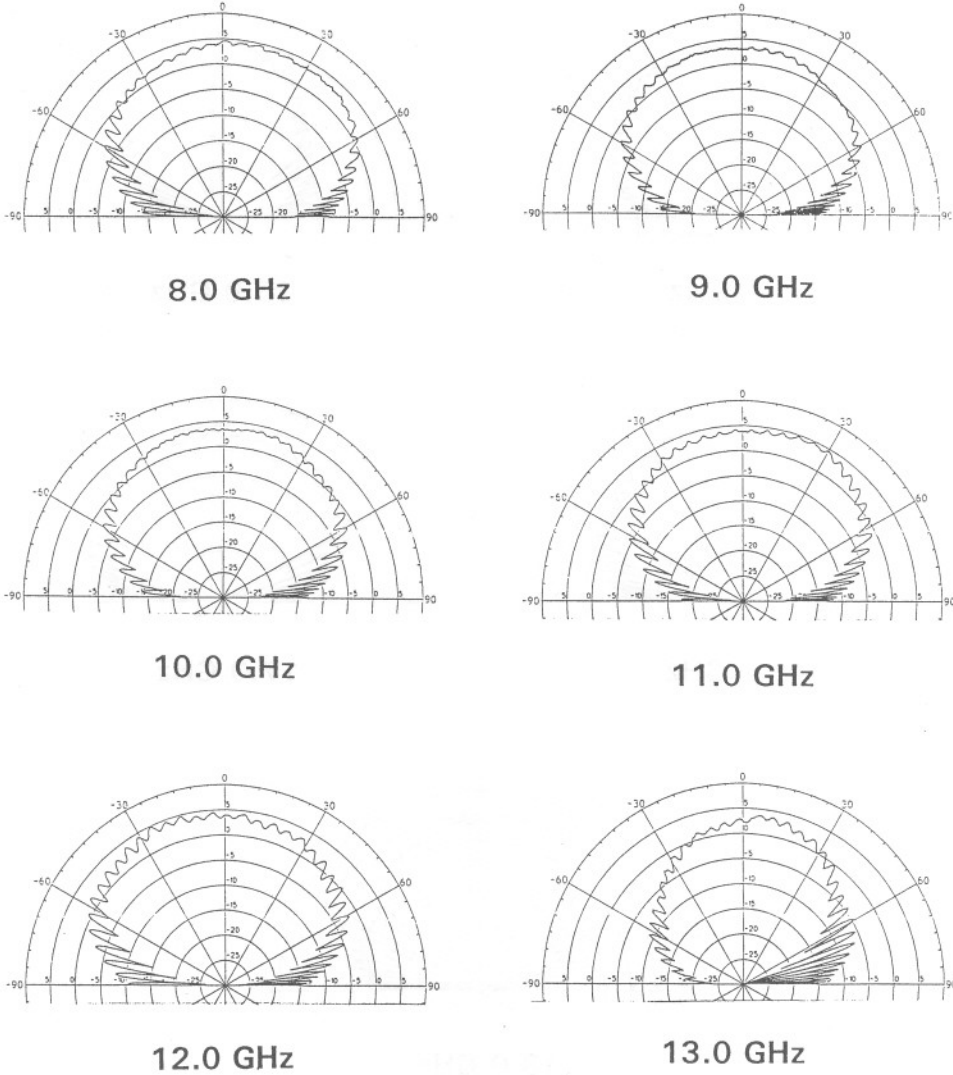
Figure 5(b).

very narrow bandwidth. Since the motive for research in the spiral antenna has been largely for ultrawide bandwidth, practical mode 2 excitation has since 1960 been carried out by using spirals with at least four arms and fed by matrix networks using hybrids and phase shifters (Corzine, 1990).

Although mode 0 has been mentioned as the case in which all the spiral arms are excited in equal amplitude and phase, it has remained largely a mathematical concept for multimode spirals. The reason why mode 0 was not implemented earlier was because the spiral arms excited with the same phase and amplitude constitute null generators between them and thus transmit and receive no power unless some meaningful "ground" can be established to facilitate the provision of the excitation voltage. The techniques used by Kaiser (1960), Donnellan (1960), and Yamauchi et al. (1994) for mode 2 could conceivably be used for excitation of mode 0 except for their narrowband nature.

14.0 GHz

15.0 GHz

16.0 GHz

17.0 GHz

18.0 GHz
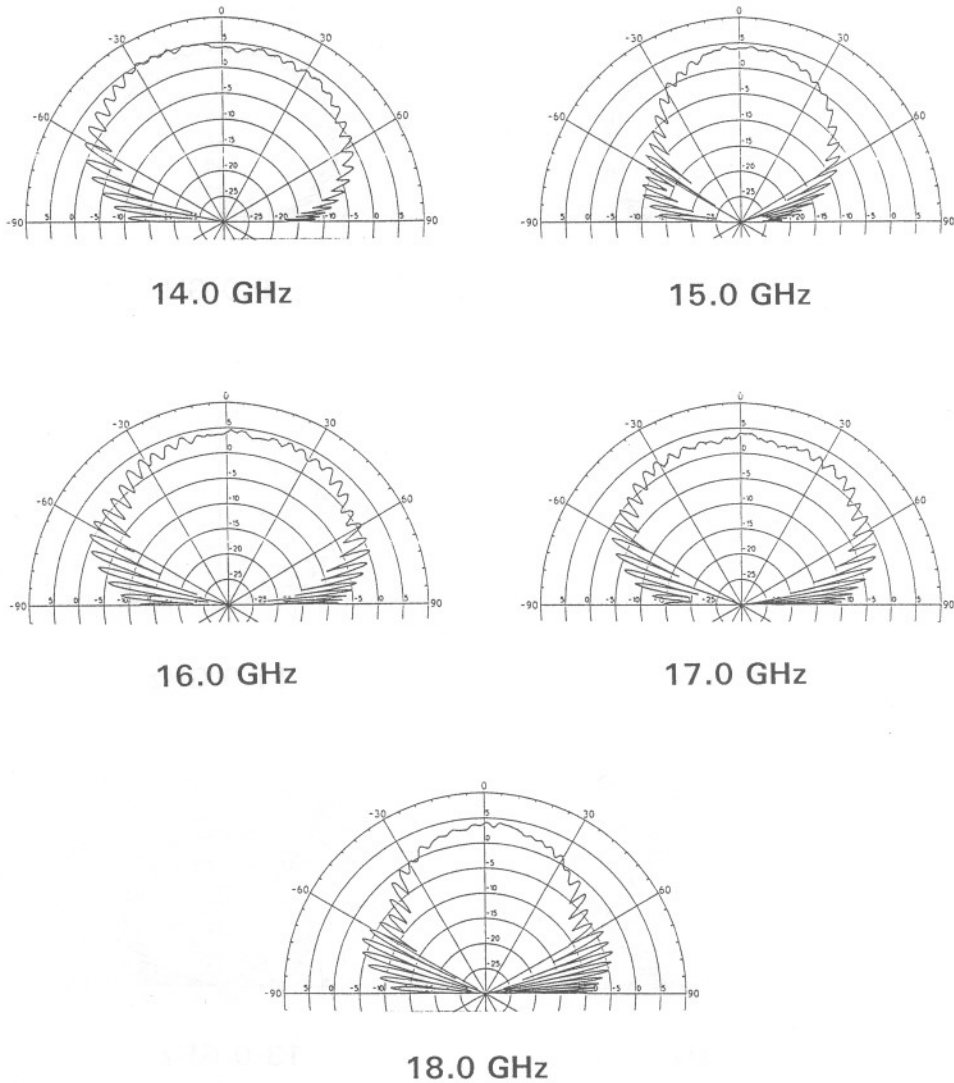
Figure 5(c).

Now, for the SMM antenna, mode 0 operation is meaningful and practical because signals with equal voltage and phase on all spiral arms can now be referenced to a common ground plane inherent in the SMM antenna, as shown in Figure 6. As a result, the techniques for extracting various modes, including that for mode 0, was investigated (e.g., Wang, 1997). Significantly, it is not mode 2 because it can be excited on a spiral with circumference less than $2\lambda_1$, the minimum size required for mode 2. Furthermore, in the case of a four-arm spiral, the mode 2 excitation would have (0°, 180°, 360°, 540°), or equivalently (0°, 180°, 0°, 180°), for arms No. 1–4; while a mode 0 excitation is (0°, 0°, 0°, 0°).

As pointed out earlier, for mode 0 operation the impedance formula in (1) is not applicable and no theory or empirical formula for its impedance exists. Therefore, our study has been largely empirical, and we have developed several experimental mode 0 SMM antenna
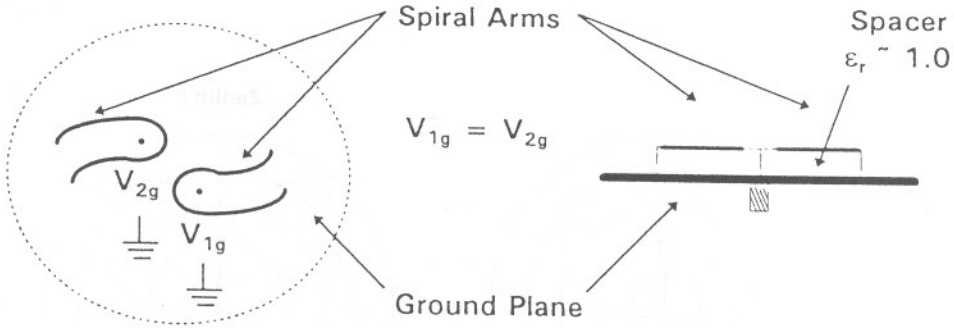
**Figure 6.** Top and side views of an SMM antenna mode 0 excitation.
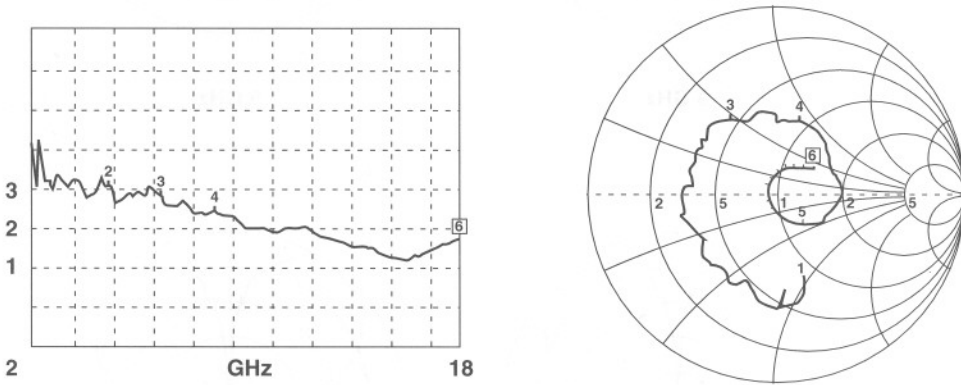
Figure 7. Measured VSWR and Smith chart display of a mode 0 SMM antenna.

models, all of which demonstrated multioctave bandwidth for both impedance and pattern. One mode 0 model is made of a two-arm spiral of 2.5-inch diameter with both spiral arms connected to the center conductor of a 50-ohm feed line via an OSM flange mount connector attached to the ground plane. The ground plane is 6 inches in diameter and is spaced $\frac{1}{8}$ inch below the spiral by using, as a spacer, a honeycomb sheet with a dielectric constant of near unity.

Figure 7 shows the measured VSWR and Smith chart display over 2–18 GHz for this model. As can be seen, a fairly constant and stable impedance, referenced to 50 ohms, over a 9:1 frequency band is achieved. The higher VSWR at the low end of the frequency band is believed to be due to reflections from the edge of the spiral. Note that no impedance matching technique has been applied to this antenna, thus the impedance shown in Figure 7 represents the impedance of the antenna per se. Therefore, further improvements in impedance matching can be readily realized by internal matching in the feed network using standard matching techniques, by increasing the diameters of the spiral and ground plane, and by improved reactive matching at the edge of the spiral; the latter two techniques are especially effective at the antenna's lower operating frequencies.

As important, this mode 0 model exhibits good, stable radiation patterns over a multioctave bandwidth. Typical radiation patterns are given in Figure 8. Please note that the "noise"

5 dB/div

Zenith 0

3 GHz   6 GHz

10 GHz   12 GHz
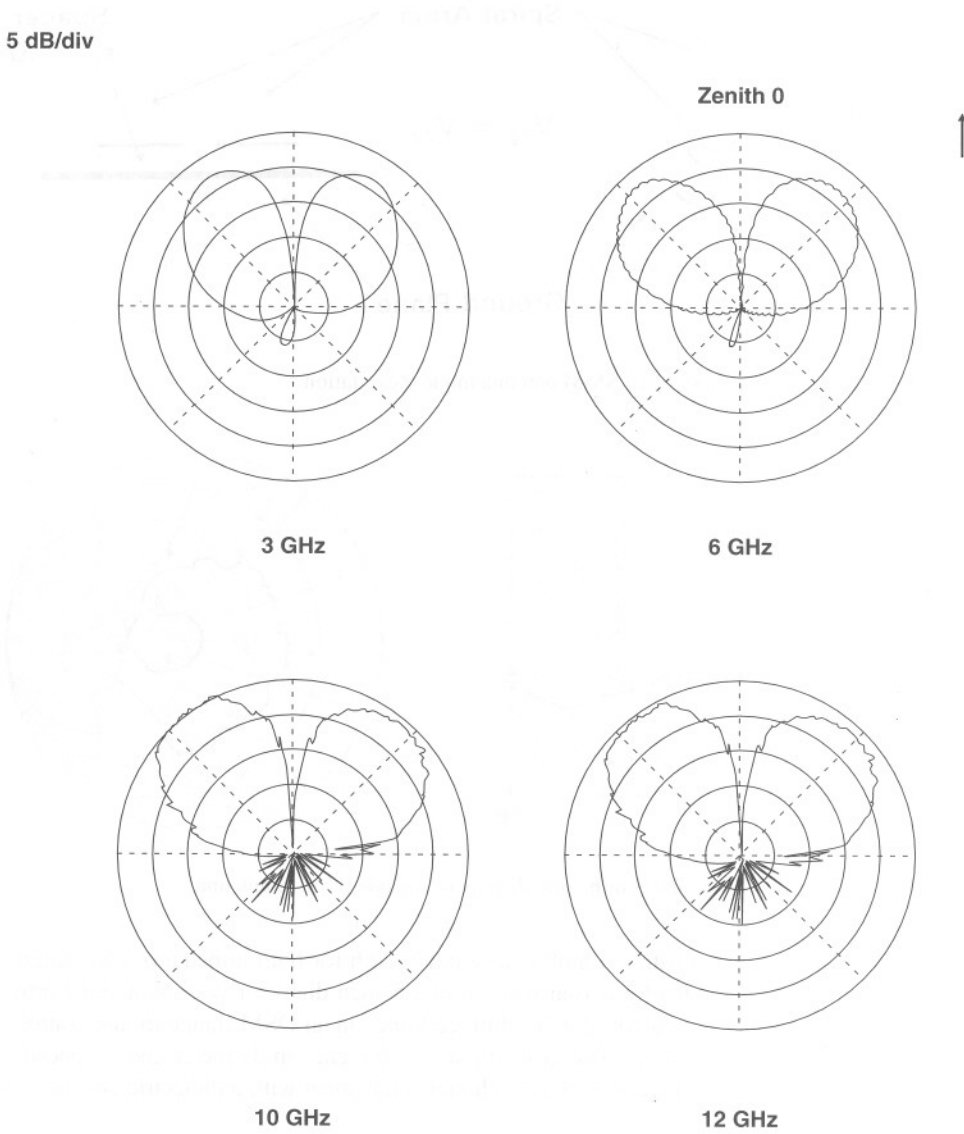
Figure 8. Measured rotating-linear patterns of a mode 0 SMM antenna.

seen in the patterns, which increases with frequency, is due to a problem with the amplifier used during the measurements, not the antenna. As can be seen, these mode 0 radiation patterns resemble somewhat the radiation pattern of a monopole on a finite ground plane, on one hand, and that of a mode 2 spiral on the other hand. The SMM mode 0 model can be adjusted to some extent to have amplitude patterns that resemble that of either the monopole or the mode 2 spiral. Techniques to increase the gain near the ground plane were also developed.

IAPS for Phased Arrays

The integrated antenna/phase-shifter (IAPS) combines the SMM antenna element and the phase-shift mechanism inherent in the spiral into a single simple-phased array module. The progress of this research has been partially presented before (e.g., Wang et al., 1996). The inherent phase pattern of the spiral element allows the phase front to be shifted by rotating the spiral either electronically or photonically.

Several prototype 3-bit element models have been designed, fabricated, and tested over two different frequency bands. Figure 9 shows the measured phase for the 8 states (0°, 45°, 90°, 135°, 180°, 225°, 270°, and 315°) of a 3.75″-diameter model over the 1.0 to 10.0 GHz band. As can be seen, the phase errors for all states of both models are well under $\frac{1}{2}$ bit, therefore sufficiently accurate for ordinary-phased array applications. Note also that a 3-bit phase-shifter is adequate for phased arrays in most applications.

In addition to the phase measurements performed, VSWR and radiation patterns of the 3-bit models were also recorded. Typical VSWR data for the 8 states of the 3.75″ model are shown in Figure 10. As can be seen, the VSWR shows good broadband impedance matching, typically being below 3:1 over a 10:1 band (VSWR being slightly higher at the higher end of the bands). The model also exhibited good pattern quality over the 10:1 band, and gain measurements made over the 5–6 GHz range indicate a gain of about 3 dbi. Since the directivity of the antenna is about 6 dBi, the 3 dBi measured gain implies a 3 dB total loss, which includes losses in the antenna aperture and the feed network including the phase switching devices.

We have also constructed a 3-element array using this 3-bit IAPS. A substantial number of measured radiation patterns were recorded, covering each of the 8 possible states for each
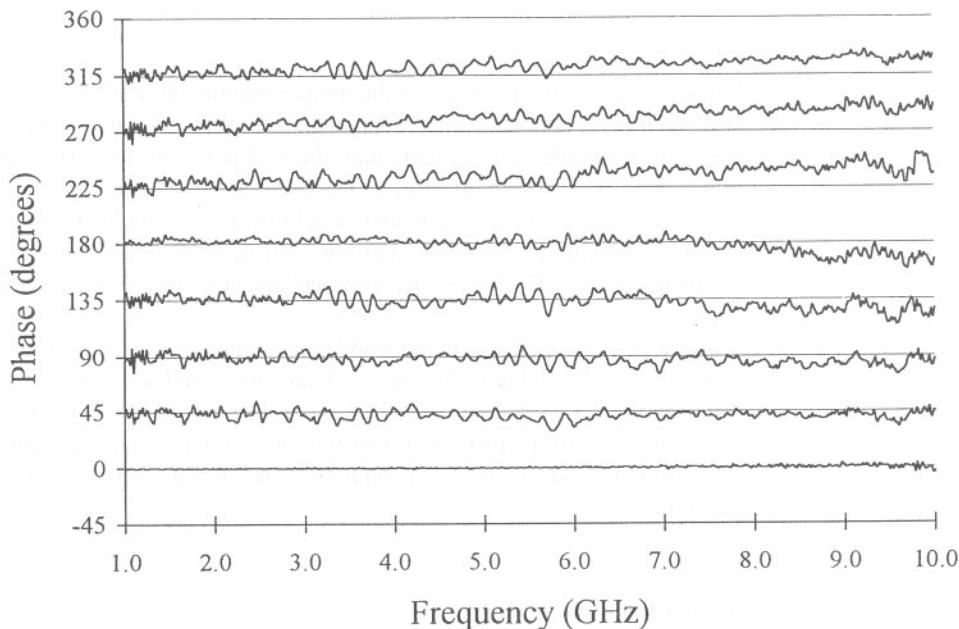
Figure 9. Measured phase shifts for a 3.75″-diameter 3-bit SMM antenna/phase-shifter.
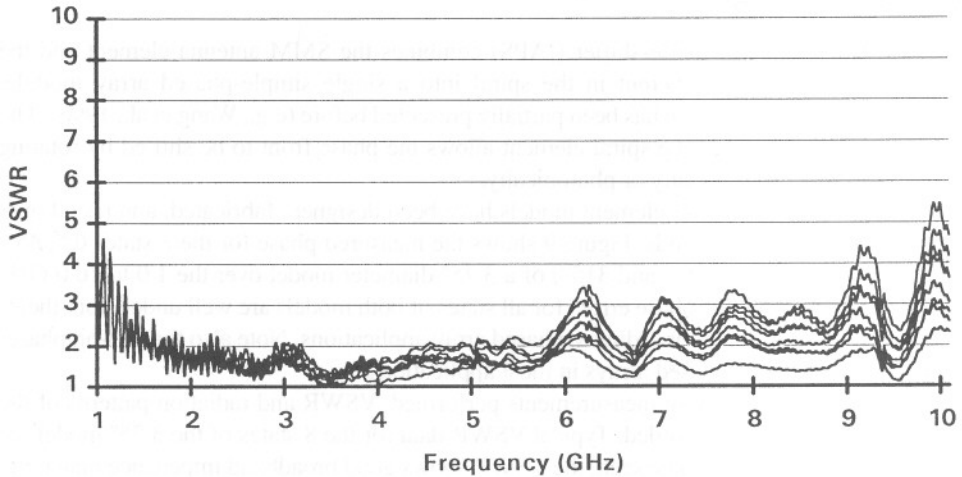
Figure 10. Typical VSWR data measured for a 3.75″-diameter 3-bit SMM antenna/phase-shifter.

element at 100 MHz increments over the frequency range of 1.0 to 10.0 GHz. These were compared with calculated radiation patterns and found to be in good agreement with each other. Figure 11 shows a typical example of agreement between these calculated and measured radiation patterns at 1.7 GHz for scan angles of 0°, −9°, −22°, and −35°.

Other Applications

Considerable research has been performed to harness the unique multimode, multipolarization features of the spiral antenna for applications in radar and telecommunication to achieve multifunction, real-time switched modes, etc. In particular, the first practical (low-cost and low-battery-power consumption) personal smart antenna using the SMM antenna has been developed (Tillery et al., 1999). The sensing, control, and switching circuits employ CMOS-FET technology, which achieved high performance and low cost in 1998. Further performance and cost improvements using MEMS (microelectromechanical systems) devices are expected.

Although this paper focuses on applications in radar and telecommunications, it is important to state that in theory the spiral as a high-efficiency TW antenna could achieve pattern quality as good as the conventional dissipatively matched spiral antennas, especially when flush-mounted on a platform. Platform-compatibility and low noise temperature, and thus range of detection, are also important advantages of the high-efficiency spiral antenna as compared with conventional spirals.

Issues of Efficiency and Pattern Stability

Although highly satisfactory performance has been achieved for the high-efficiency SMM antenna, the following two issues have been raised by some:

———— Measured

- - - - - - Calculated

5 dB/division
All measurements at 1.7 GHz
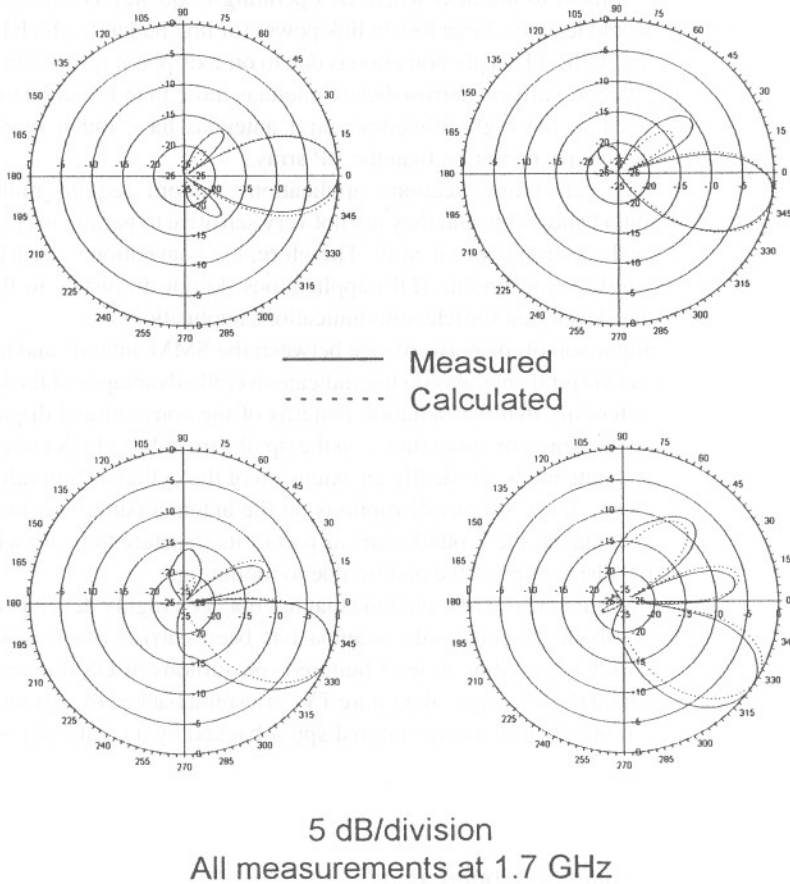
Figure 11. Measured and calculated radiation patterns at 1.7 GHz for three-element array with beam steered to 0°, −9°, −22°, and −35°.

1. observed low efficiency at the low end of the operating frequency band of the spiral antenna,
2. observed pattern stability over the frequencies of operation being inferior to that of the dissipatively loaded spiral.

We will comment on these two issues as follows.

Pattern Stability

It must be pointed out that the issue of pattern stability is largely from the perspective of the conventional receive-only spiral antennas in military applications such as direction finding. To illustrate this point, it is worth pointing out that the ultrabroadband LP antennas (widely used in TV reception and telecommunications) suffer from much more severe irregularities in their radiation patterns over their operating bands. In particular, they have pattern ripples of up to 1 dB in their main beam at some frequencies due to their discontinuity in radiation zone that

shifts from one dipole element to the next when the operating frequency is changed; these seemingly minor dips would lead to a large loss in link power (or link budget), which has been observed to be as large as 20 dB. (This phenomenon is due to on-axis phase reversal in its radiation pattern, which apparently affects narrow-beam antennas more than broad-beam antennas.) Our observation is that the high-efficiency spiral antennas have much more stable patterns across their multioctave operation than the LP array.

More fundamentally, telecommunications applications seldom require multioctave instantaneous (continuous) bandwidth, and they are not very sensitive to pattern irregularities, especially in the multipath environment on earth. Therefore, the conventional yardsticks for spiral antennas based on direction finding (DF) applications do not do justice to the high-efficiency spiral antennas developed for telecommunications applications.

Furthermore, a comparison of the performance between the SMM antenna and the commercial dissipatively loaded spiral antennas do not indicate overall advantages of the latter. At this point, it is worth reiterating that the radiation patterns of the conventional dissipatively loaded spiral antenna are measured by mounting it on the tip of a metallic cylinder of the same diameter so that the spiral antenna is physically an extension of the cylinder. Naturally, when it is mounted on a platform, fairly serious disruptions on the antenna pattern occur. On the other hand, the SMM antenna has the ground plane as part of its structure to begin with; thus there will be little, if any, disruptions of the pattern due to mounting.

In addition, the SMM antenna is a new antenna that has not been highly developed, while research in dissipatively loaded receive-only antenna has been carried out for over four decades in programs worldwide totaling at least hundreds of millions of US dollars. Therefore, there is no fundamental reason why in the future TW in a spiral backed by a ground plane could not reach a purer mode than in a conventional spiral backed by a cavity of absorptive material.

Low Efficiency at Low End of Operating Band

It must be pointed out that if the diameter and spiral-to-ground-plane spacing are adequately large, there is no problem of low efficiency for the SMM antenna at the low end of operating band (Wang & Tripp, 1991). In other words, the low-efficiency problem can be overcome by removing the restriction on the physical size of the antenna.

It was observed (Wang & Tillery, 1996) that the gain loss at low end of the operating band of the SMM antenna can be explained to be due to the dissipative losses experienced by the TW in its propagation along the spiral arms. Spirals are generally etched on a copper-clad dielectric substrate, which has a fairly lossy metallization and a substantial loss tangent in the dielectric (0.02 to 0.001 depending on the material used in the product). Recently, silver-metallized ceramic substrate (loss tangent < 0.0003) became commercially available at low cost. As a result of this one order of magnitude in reduction of conductor and dielectric losses, significant progress in efficiency and gain is being made.

Size Reduction for Spiral Antennas

As discussed in the section on "Experimental Observations and Applications," size reduction is now one of the three fundamental technical barriers in wireless telecommunications. In

addition to the initial work of Chu (1948) that established the gain/efficiency-bandwidth limitation for omnidirectional antennas of a given electrical size, considerable work driven by practical needs has been conducted by many with confirming results (e.g., Harrington, 1960; Collin & Rothschild, 1964).

It is worth pointing out that the theories that underline the gain-bandwidth limitation for a given size were all based on expansion of fields by canonical wave modes, mainly the spherical and cylindrical wave functions. It is conceivable that if exact analytical solution for problems having spiral geometry is available, the conclusion may be different. The TW antennas are generally wideband, and the spiral has inherently the largest bandwidth among TW antennas, mainly because the geometry of the spiral provides a smooth, continuous transition with no parallel in the Euclidean space. In nature, many biological, geophysical, and astronomical structures and phenomena have a spiral geometry (e.g., DNA, tornado, galaxy). The spiral geometry is key to the unusual phenomena in natural mechanical waves; the power of tornados, cyclones, and typhoons is largely derived from the spiral motion that makes it possible to generate, in a small space, the velocity and power that are not achievable by other means. It is plausible that the spiral geometry could also support electromagnetic waves offering performances that are not possible by conventional waves invariably characterized by canonical geometries.

The potential for size reduction of spiral antennas can also be argued from an intuitive perspective. The mode-1 or mode-0 spiral at its normal size is about the same in size as the resonant antennas. For example, the patch antenna has a resonant dimension of $\lambda/2$, while a mode-1 spiral needs to be large enough to contain a radiation zone having a diameter of $\lambda/3$; therefore, both antennas have approximately the same dimensions. To reduce their size, techniques used are invariably associated with some sacrifice in efficiency-bandwidth. However, since the spiral antenna has a much larger bandwidth than the resonant patch antenna to begin with, it can give up some of its bandwidth and still have a large gain/efficiency bandwidth, while the resonant patch antenna must further sacrifice its already small bandwidth as its size is reduced. In other words, since a regular spiral has about the same size as a regular patch antenna, yet has a much larger bandwidth, it follows that after both have been reduced in size and thus in efficiency, the spiral should emerge as having a larger gain/efficiency-bandwidth than the patch antenna.

Conclusions and Recommendations

As a TW antenna, the spiral has the unique feature of being physically small as compared with other TW antennas because the TW propagates along the spiral arms in a manner that is most efficient in the use of space. This feature and its platform compatibility have been exploited to develop the spiral into practical radar and telecommunications antennas. The compactness of the spiral as compared with other TW antennas cannot be overemphasized.

Furthermore, from the perspective of TWs, the high-efficiency spiral antenna is believed to have considerably more potential because of the unique geometry of the spiral. Therefore, the spiral as a TW structure offers a unique opportunity for antenna engineers in dealing with the needs of the phenomenal wireless telecommunication revolution that is being severely handicapped by the lack of suitable antennas. In addition to its wideband/multiband performance and size reduction potential, the spiral's unique geometry allows easy and powerful switching, control and various manipulations to generate performance, and special features that are difficult or even impossible by antennas of other geometries.

References

Chu, L. J. 1948. Physical limitations of omni-directional antennas. *Journal of Applied Physics* 19:1163–1175.

Collin, R. E., & S. Rothschild. 1964. Evaluation of antenna Q. *IEEE Transactions on Antennas and Propagation* 12:23–27.

Corzine, R. G., & J. A. Mosko. 1990. *Four-arm spiral antennas.* Norwood, MA: Artech House.

Deschamps, G. 1959. Impedance properties of complementary multiterminal planar structures. *IEEE Transactions on Antennas and Propagation:* S371–S378.

Donnellan, J. R. 1960. Second-mode operation of the spiral antenna. *IRE Transactions on Antennas and Propagation* 8:637.

DuHamel, R. H., & J. P. Scherer. 1993. Frequency-independent antennas. In *Antenna engineering handbook,* ed. R. C. Johnson. New York: McGraw-Hill.

Harrington, R. F. 1960. Effect of antenna size on gain, bandwidth, and efficiency. *J. of Research of NBS* (now *Electromagnetics*), *D*(1).

Kaiser, J. A. 1960. The archimedean two-wire spiral antenna. *IRE Transactions on Antennas and Propagation* 8:312–323.

Mayes, P. E. 1988. "Frequency-independent antennas." In *Antenna handbook*, ed. Y. T. Lo and S. W. Lee. New York: Van Nostrand Reinhold.

Nakano, H., K. Nogami, S. Arai, H. Mimaki, & J. Yamauchi. 1986. A spiral antenna backed by a conducting plane reflector. *IEEE Transactions on Antennas and Propagation* AP-34:791–796.

Tillery, J. K., G. T. Thompson, & J. J. H. Wang. 1999. Low-power low-profile multifunction helmet-mounted smart array antenna. In *1999 IEEE International Antenna Symposium*, Orlando, FL, July 11–16. Piscataway, NJ: IEEE Press.

Walter, C. H. 1965. *Traveling wave antennas.* New York: McGraw-Hill.

Wang, J. J. H. 1997. Improved spiral-mode microstrip (SMM) antennas and associated methods for exciting, extracting and multiplexing the various spiral modes. U.S. Patent No. 5,621,422, issued April 15.

Wang, J. J. H., & J. K. Tillery. 1996. Performance of spiral-mode microstrip (SMM) antenna and its mystery and remedy of gain loss at low end of operating band. In *1996 IEEE International Antenna Symposium,* Baltimore, MD, pp. 2042–2045, July 21–26. Piscataway, NJ: IEEE Press.

Wang, J. J. H., J. K. Tillery, G. T. Thompson, & K. E. Bohannan. 1996. A multioctave-band photonically controlled, low-profile, structurally embedded phased array with integrated frequency-independent phase-shifter. In *1996 IEEE International Symposium on Phased Array Systems and Technology,* Boston, MA, pp. 68–73, October 15–18.

Wang, J. J. H., & V. K. Tripp. 1991. Design of multioctave spiral-mode microstrip antennas. *IEEE Transactions on Antennas and Propagation* 39:273–276.

Wang, J. J. H., & V. K. Tripp. 1994. Multioctave microstrip antenna. U.S. Patent No. 5,313,216, issued May 17.

Wang, J. J. H., & V. K. Tripp. 1996a. Compact microstrip antenna with magnetic substrate. U.S. Patent No. 5,589,842, issued Dec. 31.

Wang, J. J. H., & V. K. Tripp. 1996b. Conformable multifunction shared-aperture antenna. U.S. Patent No. 5,508,710, issued April 16.

Yamauchi, J., K. Hayakawa, & H. Nakano. 1994. Second-mode operation of an archimedean spiral antenna backed by a conducting plane reflector. In *Electromagnetics* 14:319–327.